

Optimization of a Scroll Expander Applied to an Ammonia/Water Combined Cycle System for Hydrogen Production - Paper No. 1645

Herbert A. Ingley, PhD, PE
University of Florida
P. O. Box 116300
Gainesville, FL 32611
ingley@ufl.edu

Robert Reed
University of Florida
PO Box 116300
Gainesville, FL 32611

D. Yogi Goswami, PhD, PE
University of Florida
P.O. Box 116300
Gainesville, FL 32611
goswami@ufl.edu

ABSTRACT

The ammonia-water combined power/cooling cycle proposed by Goswami (1995) utilizes a binary ammonia/water working fluid to produce both power and refrigeration. The cycle is a combination of an ammonia-water refrigeration system and an ammonia-based Rankine cycle.

The unique ability of this cycle to produce both power and refrigeration gives rise to two advantages for use in a hydrogen economy. First, the cycle can utilize low-grade renewable heat sources such as that available from inexpensive flat plate solar collectors to produce the power needed to drive an electrolyzer and liquefier. Second, the cooling produced by the cycle can be used to pre-cool hydrogen prior to liquefaction, thereby reducing the power requirement of the liquefaction compressor equipment. In this manner renewable energy source utilization is improved compared to technologies such as wind or photovoltaic electrolysis.

The power output and cooling capacity of the cycle under given operating parameters is highly dependent on the expander efficiency. Irreversibilities due to friction and leakage decrease the amount of work extracted from the fluid. Because less work is extracted, the expander exhaust temperature is higher and the cooling capacity is reduced.

The main criteria for expander selection are operating pressures and temperatures, flow rate of ammonia vapor and material compatibility with ammonia. Ammonia is a corrosive substance that reacts with metals such as copper, brass, and bronze, all of which are commonly used as bearing or bushing material. The expander selected for use in the combined cycle must be sized correctly for the flow rate and for the operating pressure ratio for maximum

power production and refrigeration capacity. It must also be constructed out of steel, aluminum, or another material compatible in an ammonia environment. Various expander designs using unique expansion methods exist throughout industry. These designs can be organized into two categories, positive-displacement and turbo-machinery, based on the method of fluid displacement. This paper provides a comparison of these expander designs with emphasis on the scroll compressor.

1. INTRODUCTION

Current energy consumption and forecasted demand with regard to limited fossil fuel reserves is driving the necessity for the conversion to a renewable resources-based global energy market. Economical, environmental, and political factors are further motivations. Hydrogen is becoming more significant as a potential energy carrier for this renewable energy market.

Approximately 85.7% of the world's energy is currently supplied by fossil fuels, with crude oil making up 38.8% of that total. Global energy consumption is projected to increase 54% over the next 25 years (Energy Information Administration, 2004).

This increased demand is being fed primarily from countries with rapidly industrializing and emerging economies such as India and China. Proven oil reserves are sufficient to satisfy this demand over the next 20 years, after which there is debate as to whether oil production will peak before 2030 or that continued technological progress and new oil discoveries will satisfy the demand well into this century (Ramsay, 2003).

The economic effects of increasing energy demand on a limited supply are apparent today with peak 2004 oil

prices near \$50/barrel and average gas prices in the US near \$2.00/gallon. As fossil fuel production peaks and inevitably begins to decline, and without other viable energy sources, prices will continue to escalate.

Industry is affected directly and indirectly by the cost of energy. The direct effect is to increase the cost of processing raw materials and production. Fuel costs involved with transporting finished goods is the indirect effect. The natural response of industry to increasing cost is to slow production and/or reduce labor forces, thus slowing the entire economy.

A number of adverse environmental phenomena such as the greenhouse effect, air pollution, acid rain, and oil spills are attributed to the use of fossil fuels. The burning of all fossil fuels produces carbon dioxide, a greenhouse gas. The Energy Information Administration reports that carbon dioxide contributes over 84% to the total of greenhouse gases emitted (Mirabal, 2003). Global warming is widely debated as an ongoing occurrence, but if it were found to be so, carbon dioxide emissions would be the main cause.

Another by-product of fossil fuel combustion in air is the formation of nitrogen oxides (NOx) that contribute to ozone depletion as well as smog formation. Complex fossil fuels, such as petroleum and coal may also contain sulfur, which form sulfides that can cause acid rain. These environmental factors and others mentioned contaminate water supplies, damage ecosystems, and are related to the occurrence of many respiratory illnesses in humans.

In 1985, the US imported 27.3% of the oil it consumed. Over the past 18 years the U.S. dependence on foreign oil has steadily increased to 56.1% and is projected to be 69.6% of that consumed by 2025 (Energy Information Administration, 2003).

With greater dependence on foreign oil, the U.S. will be reliant on a stable Middle East, Russia, and South America. International crises such as those recently in Iraq and Venezuela will have a more significant impact on oil prices as they do today. It is important that alternative energy sources are developed today to deal with the issues of tomorrow. Current research initiatives around the world are focused on hydrogen as the fuel of the future. With the development of a hydrogen economy based on renewable resources, greenhouse gas emissions will be reduced, the economy will be more independent of oil prices, and foreign policy will be less influenced by oil reserves.

2. HYDROGEN AS A FUTURE ENERGY CARRIER

In 2001, 20.4% of global energy consumption supported transportation; of which 96% was supplied by crude oil (Energy Information Administration, 2003). By developing an alternative fuel for transportation, world oil consumption could be reduced by as much as 19.6%. Reducing oil consumption likewise reduces greenhouse

emissions and ozone depletion. Hydrogen holds promise as the fuel to achieve these goals because it can be produced from water using renewable energy sources and it burns clean; with water and heat as the only combustion products (NOx emissions are possible when burned in air).

One of the barriers to the widespread use of renewable resources is the geographical limitation. For example, hydropower can only be utilized in areas where dams can be built and solar power is dependent on incident sunlight, which varies from region to region. Renewable energy technologies can be utilized more efficiently and on a broader scale by constructing large capacity plants in regions with prominent sources of energy. The energy can subsequently be converted to chemical energy by producing hydrogen, enabling delivery to a larger market.

Governments around the world realize the potential of hydrogen as an alternative fuel. Many countries have adopted research initiatives in the production, storage, and utilization of hydrogen. The U.S. Department of Energy has recently announced plans to advance toward a hydrogen-based energy system making fuel-cell-powered vehicles available by 2010. Industry is following suit as most major automobile manufacturers have significant programs in place to develop fuel cell powered vehicles (Ramsay, 2003).

Hydrogen is a safe and clean fuel that when produced using renewable energy is virtually pollution free. Hydrogen also provides a means to convert from a fixed source of energy to one compatible with the needs of transportation. With further development of production and storage technology, hydrogen can become the primary source of fuel for the transportation sector and can help usher in the renewable energy era.

3. NOMENCLATURE

CHWS	chilled water source
CHWR	chilled water return
CWS	cooling water source
CWR	cooling water return
CO2	carbon dioxide
COP	coefficient of performance
H	enthalpy [Btu/lbm]
HHV	higher heating value [Btu/lbm]
HHWS	heating hot water source
HHWR	heating hot water return
L	liquid
LH2	liquid hydrogen
LHV	lower heating value [Btu/lbm]
LN2	liquid nitrogen
P	pressure [psia]
PV	photovoltaic
S	entropy [Btu/lbm-R]
SMR	steam/methane reformation
STP	standard temperature and pressure

T	temperature [$^{\circ}$ R or $^{\circ}$ F]
V	volts [V] or volumetric flow rate [cfm]
X	ammonia mass fraction
g	vapor
h	enthalpy [Btu/lbm] or hour [hr]
m	mass flow rate [lbm/hr]
v	specific volume [ft ³ /lbm]
w	specific work [kW/lbm]
x	mass flow ratio
y	liquid yield ratio
z	nitrogen requirement ratio
β	coefficient of thermal expansion
ϵ	heat exchanger effectiveness
η	efficiency
μ JT	Joule-Thompson expansion coefficient
μ s	isentropic expansion coefficient
ρ	density [lbm/ft ³]
ω	rotational speed [rad/s]

Subscripts

CW	cooling water
H ₂	hydrogen
NH ₃	ammonia vapor
P	isobaric or pump
T	isothermal
ab	absorber
act	actual
ad	adiabatic
c	compressor
cool	cooling load
e	expander
f	liquid
g	electric generator
h	isenthalpic
in	expander gas inlet
max	maximum
min	minimum
o	standard conditions
opt	optimum
out	expander gas outlet
rect	rectifier
s	isentropic
shaft	expander pulley shaft
strong	high ammonia concentration stream
th	thermoneutral
v	volumetric
vg	vapor generator

4. THEORETICAL BACKGROUND

Hydrogen is the simplest, most abundant element in the universe comprising 75% of all visible matter by mass (Flynn, 1997). Currently, the majority of the hydrogen produced in the U.S. is used as a chemical in a variety of commercial applications including ammonia production,

hydrogenation of fats and oils, and methanol production (National Hydrogen Association, 2004).

Hydrogen has several characteristics that make it a desirable alternative fuel for transportation:

- Highest energy content per unit mass of any known fuel (51,574 Btu/lbm) hydrogen produces 2.7 times more energy per unit mass than gasoline when burned.
- Clean – combustion of hydrogen produces no carbon dioxide or sulfur emissions. When burned with oxygen, the only byproducts are water and heat. If burned in air, nitrogen oxides may be produced.
- Renewable – hydrogen can be produced by a variety of methods using renewable energy sources for a virtually limitless and pollution free fuel supply.
- Technologically compatible – in the 1920s, German engineer Rudolf Erren successfully converted IC engines to hydrogen burning engines (National Hydrogen Association, 2004). Hydrogen can also be reacted with oxygen in a fuel cell to produce electricity to drive a motor.
- Efficient utilization – hydrogen IC engines are about 25% efficient, fuel cells are 45-60% efficient; typical gasoline IC engines are 18-20% efficient (National Hydrogen Association, 2004). Hydrogen fuel cell powered vehicles can be up to three times more efficient than today's gasoline engines.

The U.S. currently produces 9 million tons or 3.2 trillion cubic feet (90 billion Nm³) of hydrogen per year. Of this amount, 95% is produced by steam/methane reformation (SMR) (National Hydrogen Association, 2004). SMR operates by reacting a natural gas feedstock with steam at high temperatures (700 – 925 $^{\circ}$ C) to produce carbon monoxide and hydrogen. The carbon monoxide is then consumed in a water/gas shift reaction to create CO₂ and additional hydrogen. Other hydrogen production methods are outlined in Figure 4.1.

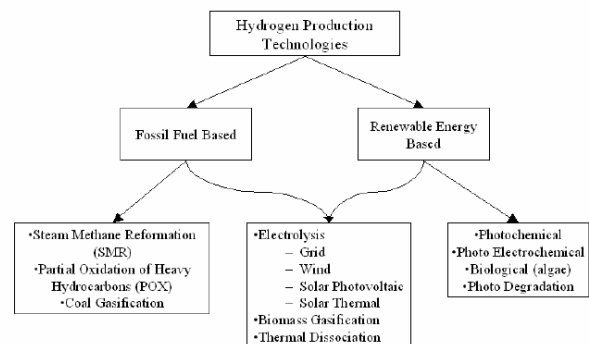


Figure 4.1 Hydrogen production technologies by energy source

Detailed descriptions of each fossil fuel based production technology are given by Mirabal (2003).

SMR is currently the most cost effective method of producing hydrogen; however, because of increasing fossil fuel cost due to diminishing supplies and reduced capital cost of renewable energy due to technological improvements, wind and ammonia/water combined power/refrigeration cycle solar power based electrolysis are projected to become the most cost competitive by 2020 (Mirabal, 2003).

Table 4.1 Projected hydrogen costs of various production methods¹

Year	Hydrogen Production Costs (\$/lb)			
	2003	2010	2030	2050
Steam Methane Reformation	0.66	0.90	2.75	9.88
Partial Oxidation	0.80	0.90	1.44	2.89
Coal Gasification	1.12	1.20	1.65	2.83
Electrolysis - Grid Power (fossil fuel based)	1.53	1.63	2.42	4.12
Electrolysis - PV / Antenna Power	3.47	2.40	0.91	0.65
Electrolysis - Wind Power	1.33	1.14	0.78	0.60
Electrolysis - Ammonia Water Combined Cycle	2.50	1.37	0.89	0.63

¹ Original data converted from \$/GJ using the HHV of hydrogen (Mirabal, 2003)

Although there are other methods available to produce hydrogen from renewable resources, electrolysis is the most versatile and technologically developed. Electrolyzers do not require high temperature for operation as do thermal decomposition, dissociation, or chemical processes nor are they dependent exclusively on sunlight. For these reasons, electrolysis is expected to be the predominate method of hydrogen production in a future hydrogen economy.

One of the barriers preventing the wide use of hydrogen as a fuel is its storage. This issue centers on hydrogen's low density and correspondingly low energy density.

Because of its low density, hydrogen requires a large volume for an equivalent amount of stored energy as compared to other common fuels. To illustrate this fact, the energy equivalent of 10 gallons (37.85 liters) of gasoline would require a tank size of 175 gallons (662.4 liters) for gaseous hydrogen at 3000 psig and 37.6 gallons (142.3 liters) for liquid hydrogen. Another issue with hydrogen storage in regards to its use as a motor fuel is the combined weight of the container, safety equipment and any required insulation.

Container weights (including fuel) for several hydrogen storage methods are given for an energy equivalent of 7.93 gallons (30 liters) of gasoline in Figure 4.2.

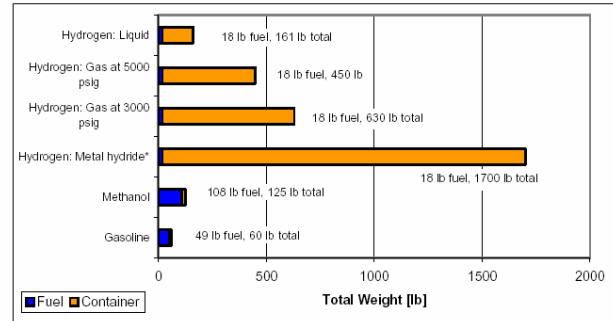


Figure 4.2 Fuel and total weight of several hydrogen storage systems.

*Storage capacity by weight approximately 1.1%.

There are several methods of hydrogen storage currently available or being researched. They are summarized as follows:

Metal hydrides. Metal hydrides are specific alloys consisting primarily of granular magnesium, nickel, iron, and/or titanium. These alloys are capable of adsorbing hydrogen (1% - 8% by weight) at high pressure and moderate temperature and releasing it under low pressure and elevated temperature. Metal hydrides are characterized by de-adsorption temperature. Low-temperature (< 200 °F) hydrides operate at higher pressures to prevent hydrogen release at ambient temperatures. These hydrides typically adsorb 1 -2 percent of their weight in hydrogen. Higher temperature (> 250 °F) hydrides hold 5 -10 percent hydrogen by weight, but require significant amounts of heat to attain the temperatures required to release the stored hydrogen. (Sunatech Inc., 2001).

Metal hydrides provide the safest means of storing hydrogen. Because the hydrogen is stored in a solid-state media, it cannot be ignited until released. In addition, the hydrogen is released at low pressures and moderate temperatures; therefore, no specialized storage tank is required to deal with high pressures or cryogenic temperatures.

Despite these advantages, metal hydrides are undesirable for use in transportation. Large, heavy, and costly storage units are required to hold equivalent amounts of energy as current gasoline tanks, as shown in Figure 4.2. Common hydrogen impurities such as oxygen and water reduce the ability of the tank to store hydrogen as they bond permanently to the metal. Additionally, vibrations due to typical driving conditions can result in particle attrition that also reduces the tank's useful life.

Compressed hydrogen. Compressed hydrogen is the simplest and one of the most common methods of hydrogen storage and transportation. Even at 10,000 psig, however, compressed hydrogen contains nearly 8 times less energy per unit volume than gasoline (not including the energy expended in compressing the hydrogen). Cylinders tend to

be heavy because of the robust construction necessary to withstand the high pressures and impacts. These factors make compressed hydrogen storage suitable for only short ranged applications or as a reserve fuel for liquid hydrogen powered vehicles.

Liquefied hydrogen. Liquid hydrogen is formed by cooling hydrogen gas to -423°F (-253°C) at atmospheric pressure. Storage of such low temperature fluids is achieved using a dual-walled cylinder with an evacuated space between the cylinder walls (Dewar's flask). Due to the relatively high surface to volume ratio typical of the small tanks used in transportation applications, additional multi-layered radiation insulation sheets are also employed (Flynn, 1997).

There are several technological challenges that must be overcome in order for liquefied hydrogen storage to come into widespread use. First is safe tank design to reduce weight and hydrogen boil off due to heat gains. The imperfect insulation of the inner tank supports, among other factors, causes a typical boil off rate of 3% per day (Clean Energy Research Center, 2003). Furthermore, improved methods of hydrogen liquefaction must be developed to reduce LH2 cost. Today, about 30% of the energy contained in LH2 is consumed by the liquefaction process (Fuel Cell Store, 2003).

Lastly, re-filling stations must be developed such that the public can operate them safely. Liquefied hydrogen (LH2) is currently the optimum hydrogen storage method for vehicles in terms of tank size/weight and energy density. LH2 has the highest volumetric energy capacity of any commercially available storage system being only four times less than gasoline; and because hydrogen burns more efficiently than gasoline, LH2 tanks are not necessarily four times the size of typical gasoline tanks for a given vehicle range. This allows automobile manufactures to continue using current vehicle designs, easing the transition into a hydrogen economy.

Carbon nanotubes and glass microspheres. Carbon nanotubes store hydrogen in microscopic surface pores and within the tube structures via adsorption. The mechanism by which they store and release hydrogen is similar to metal hydrides, however carbon nanotubes are lighter, cheaper, and are capable of storing 4.2 to 65% hydrogen by weight (Fuel Cell Store, 2003). Carbon nanotubes are still under research and development and currently store between one and ten percent hydrogen by mass (Clean Energy Research Center, 2003).

Glass microspheres are currently being researched as a potential hydrogen storage method. Hydrogen is stored by first warming the tiny glass spheres to increase their surface permeability and then immersing them in high-pressure hydrogen gas. The spheres are then cooled, locking the hydrogen inside of the glass balls. Increasing the temperature of the spheres reverses this process. Experiments to increase hydrogen release rates by crushing

the spheres are also being performed. The key advantage of glass microspheres is storage at ambient temperature.

The technology exists today for the introduction of hydrogen-powered vehicles; however, the size, weight, and/or cost limitations imposed on storage systems by the low energy density of hydrogen must first be overcome. Liquid hydrogen holds the greatest promise for hydrogen-powered vehicles. These storage systems have the lowest weight and volume of those commercially available, and with improved tank design and hydrogen liquefaction methods, the relatively high costs will lessen over time.

Ammonia-Water Combined Power/Cooling Cycle

The ammonia-water combined power/cooling cycle proposed by Goswami (1995) utilizes a binary ammonia/water working fluid to produce both power and refrigeration. The cycle is a combination of an ammonia-water refrigeration system and an ammonia-based Rankine cycle.

An ammonia-water mixture is used because of its desirable thermodynamic properties. Binary mixtures have varying boiling points depending on the concentration of the more volatile species. This characteristic gives a good thermal match with a sensible heat source, thereby reducing the irreversibility associated with heat transfer (Hasan, Goswami, 2003). Additionally, the low boiling point of ammonia allows the utilization of low temperature heat sources such as low-grade waste heat from industrial processes, solar water heaters, and geothermal sources. In a theoretical investigation performed by Tamm et al., the cycle is shown to operate with heat source temperatures as low as 116.6°F (47°C) albeit with low first law efficiency ($\sim 5\%$). When operating with a heat source temperature of 224.6°F (107°C) and idealized parameters, however, second law efficiencies greater than 65% are possible (2003).

The unique ability of this cycle to produce both power and refrigeration gives rise to two advantages for use in a hydrogen economy. First, the cycle can utilize low-grade renewable heat sources such as that available from inexpensive flat plate solar collectors to produce the power needed to drive an electrolyzer and liquefier. Second, the cooling produced by the cycle can be used to pre-cool hydrogen prior to liquefaction, thereby reducing the power requirement of the compressor. In this manner renewable energy source utilization is improved compared to technologies such as wind or PV electrolysis.

Process Description

Figure 4.3 gives a schematic of the cycle showing state points and flow paths. The fluid leaves the absorber at state 1 as a saturated solution at the cycle low pressure with a relatively high ammonia concentration. It is pumped to the system high pressure (state 2) before traveling through the recovery heat exchanger where it absorbs heat from the weak solution returning to the absorber. The solution is then partially boiled in the vapor generator by the heat source

producing saturated ammonia vapor and relatively weak concentration ammonia-water saturated liquid. The weak solution leaves the vapor generator at state 4 and rejects heat to the high concentration stream before it is throttled to the system low pressure and sprayed into the absorber. The rectifier cools the saturated ammonia vapor to condense out any remaining water. The vapor is then superheated to state 7 and expanded to produce work. The sub-ambient exhaust vapor (state 8) provides refrigeration before returning to the absorber where it is re-absorbed into the weak solution. The heat of condensation is rejected to the low-temperature source and the cycle repeats.

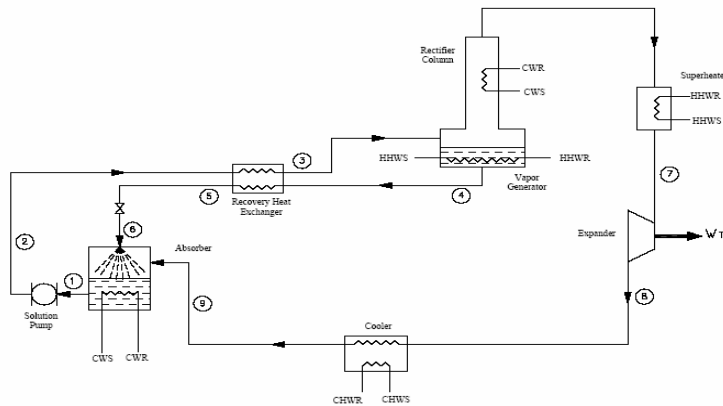


Figure 4.3 Combined cycle flow diagram

The power output and cooling capacity of the cycle under given operating parameters is highly dependent on the expander efficiency. Irreversibilities due to friction and leakage decrease the amount of work extracted from the fluid. Because less work is extracted, the expander exhaust temperature is higher and the cooling capacity is reduced. Losses in the expander have the greatest impact on the overall cycle efficiency (Tamm et al., 2003), so it is important to select an optimal design.

The main criteria for expander selection are operating pressures and temperatures, flow rate of ammonia vapor and material compatibility with ammonia. Ammonia is a corrosive substance that reacts with metals such as copper, brass, and bronze, all of which are commonly used as bearing or bushing material. The expander selected for use in the combined cycle must be sized correctly for the flow rate and for the operating pressure ratio for maximum power production and refrigeration capacity. It must also be constructed out of steel, aluminum, or any other material compatible in an ammonia environment.

Expander Design

An expansion device extracts mechanical energy from a fluid by expanding it from a high to a low pressure and converting it into shaft work. Various expander designs

using unique expansion methods exist throughout industry. These designs can be organized into two categories, positive-displacement and turbo-machinery, based on the method of fluid displacement.

Positive-displacement expanders

Positive-displacement machines such as reciprocating and rotary piston, rotary vane, and screw operate by expanding a fixed volume of fluid per oscillation. Torque pulsation is a common phenomenon due to the inherent discontinuity associated with the finite number of pistons or lobes and fixed displacement. Reliability is an issue with positive-displacement machines because of a greater number of moving parts (i.e. piston linkages, sliding vanes); and in the case of pistons, a lubrication system to reduce leakage encountered in the gap between the moving seals and volute.

Turbo-machinery

Turbo-machinery, comprised of axial and radial flow turbines, utilizes the pressure differential across a series of radial blades to provide a “lift” force to turn the rotor, thereby producing shaft work. In this manner, a continuous power output is provided. Reliability is improved over positive-displacement expanders because the rotor is the only moving part. Turbines are designed with a clearance between the blade tips and the volute to allow free rotation; however, leakage at the tips (windage loss) is the primary cause of irreversibility in the expansion process. Blade tip clearances remain approximately constant for varying turbine size. As turbine size is decreased, the loss due to windage as a percentage of the work output becomes increasingly significant. For this reason, positive-displacement expanders are more suited for small-scale operations. The amount that the blade tip clearances can be reduced is limited by the centrifugal force and/or thermal expansion of the blade material. Typical turbine operating speeds range from a few thousand up to tens of thousands RPM. Centrifugal force is dependent on blade tip speed, which is function of the RPM and the rotor diameter. As a result, larger turbines suffer greater radial blade deformation and are less suited for blade tip clearance reduction.

Scroll compressor/expander

The scroll compressor was first invented by Léon Creux in 1905 (Gravesen and Henriksen, 2001). Commercial interest in the technology was not strong until the introduction of computer numerically controlled (CNC) machines in the 1970s. CNC machines provided the basis for machining the precise elements needed for a scroll compressor to operate efficiently and quietly (Copeland corp., 2001). A scroll compressor consists of two identical spiral elements assembled with a 180° phase difference. During operation, one scroll remains stationary and the other is attached eccentrically to a motor shaft. This configuration allows the scroll to rotate in an orbiting

motion within the fixed scroll. The phase difference between the two scrolls is maintained using an anti-rotation device, typically an Oldham coupling (Copeland corp., 2001).

The fluid flow path within a scroll compressor or expander is described by Figure 4.4. As the rotating scroll orbits about the fixed scroll, the outer periphery forms a line of contact with the fixed scroll, capturing a crescent shaped volume of gas (step 1). The gas is forced toward the center discharge port in steps 2 thru 5 and compressed due to the decreasing volume of the crescents.

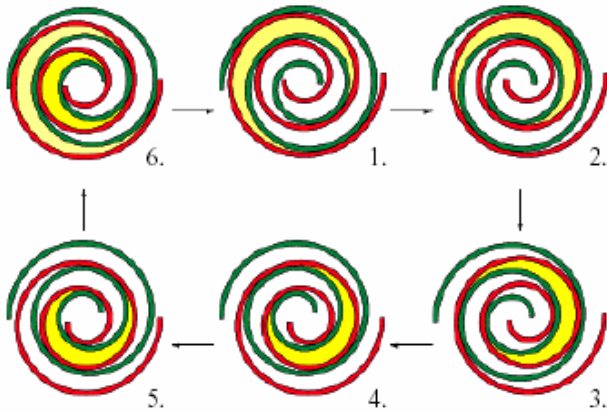


Figure 4.4 Flow path of a single fluid pocket through a scroll compressor (Adapted from Gravesen and Henriksen, 2001)

Because several of these gas pockets are being compressed simultaneously, as depicted in step 6, torque pulsation common with other positive-displacement machines is low.

Scroll compressors have been widely adopted by the HVAC industry because of the advantages they offer, including: simplistic design (i.e. fewer moving parts), low friction, low torque pulsation, and compliance. Because of their unique geometry, scrolls do not require valves or valve actuators; furthermore, there are no linkages or sliding vanes. The relative rolling motion of the contact points offers less resistance than sliding friction. Additionally, the rolling contacts provide a seal such that large volumes of oil used as a sealant are not required and leakage is reduced (Copeland corp., 2001). Continual compression process of the scroll results in a smoother power output and consequently less noise and vibration than piston-type devices. Compliance mechanisms balance the dynamic pressure and centrifugal forces in order to maintain proper sealing. These loading mechanisms correct tolerances as the scroll surfaces wear and allow the scroll elements to separate slightly in the axial or radial directions in response to a sudden pressure spike (axial compliance) or the presence of small amounts of debris or liquid (radial compliance). Taken together, these attributes contribute to

the fact that scroll compressors typically have 10% higher mechanical efficiencies than comparably sized piston compressors (Wells, 2000) and less leakage than other compressors in its class (Schein and Radermacher, 2001).

The literature suggests the potential use of a scroll compressor as a high efficiency expander (Wells, 2000). Copeland® compressors have been used successfully as expanders with R-134A and R-245FA refrigerants as the working fluid. Efficiencies over 70% were demonstrated when operated with pressure ratios between three and five (Warner, Wayne – Copeland Corporation, Personal Conversation, 10 May 2004). Scroll expanders have also been utilized in an organic Rankine micro combined heat and power system patented by Yates et al. in 2002 (US Patent and Trademark Office, 2002).

5. RESULTS AND DISCUSSION

Ammonia-water Combined Cycle

The ammonia-water combined cycle was analyzed for a fixed power output to observe the impact of expander efficiency on the heat and work requirements as well as the cooling capacity. The simulation was run under the assumptions listed previously while varying the expander isentropic efficiency from 10 to 100% in 10% increments. Results of the simulation are given in Figures 5.1 thru 5.5. The ammonia vapor mass flow rate required to drive the expander and produce 5kW of electricity is a function of only the exhaust enthalpy at state 8; since the power output and specified temperatures and pressures are held constant. From the definition of isentropic efficiency, the vapor mass flow scales with $1/\eta_e$. The weak and strong solution flow rates follow a similar trend as shown in Figure 5.1 as they are related to the vapor flow by a constant ratio of the ammonia mass fractions.

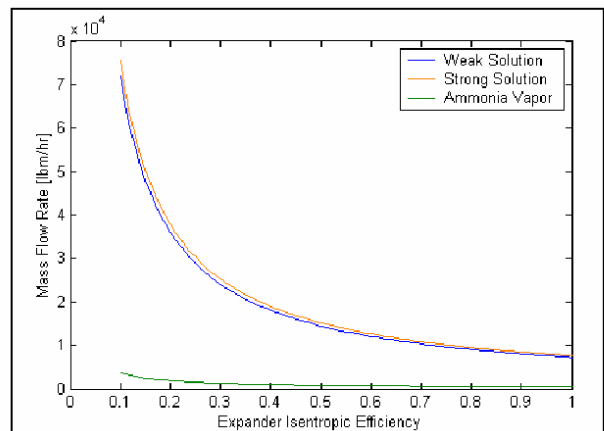


Figure 5.1 Mass flow rate dependence on expander efficiency

The maximum mass flows for the vapor, weak, and strong solutions occur at the lowest efficiency (10%) and are: 3586.34 lbm/hr (0.4519 kg/s), 72037.7 lbm/hr

(9.0767 kg/s), and 75624.1 lbm/hr (9.5286 kg/s), respectively. Likewise the minimum mass flows are (in the same order): 358.63 lbm/hr (0.0452 kg/s), 7203.77 (0.9077 kg/s), and 7562.41 (0.9529 kg/s). The mass fraction of the strong, weak, and vapor streams are $x_S = 0.3988$, $x_W = 0.3689$, and $x_V = 1.0$ (assumed). A decrease in mass flow through the system manifests itself in the reduction of work and heat interactions of the cycle for a given output as seen in Figures 5.2 and 5.3. Minimum pump work, boiler heat input and absorber heat rejection are: 0.724 Hp (0.540 kW), 331,566 Btu/hr (97.18 kW), and 321,117 Btu/hr (94.11 kW). The ideal cooling capacity under these conditions is 9130.26 Btu/hr (2.68 kW). Figure 5.4 concludes that at least 60% efficient expansion is required to obtain any cooling capacity. Below this point, the exhaust temperature of the expander exceeds the assumed temperature of the substance to be cooled (85 °F). This effect is also evidenced in the plot of the expander isentropic efficiency versus the cycle thermal efficiency (Figure 5.5).

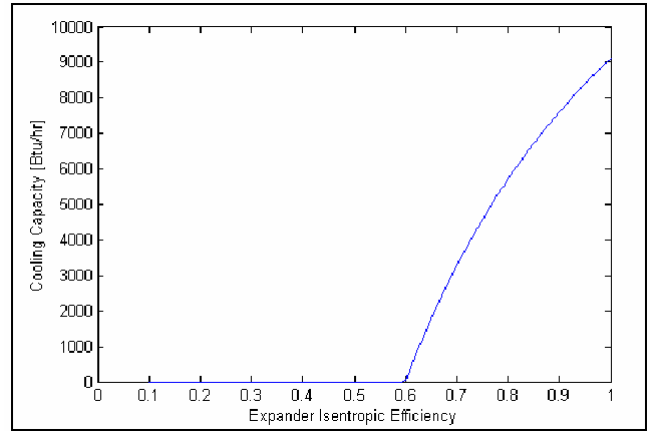


Figure 5.4 Cycle cooling capacity as a function of expander efficiency

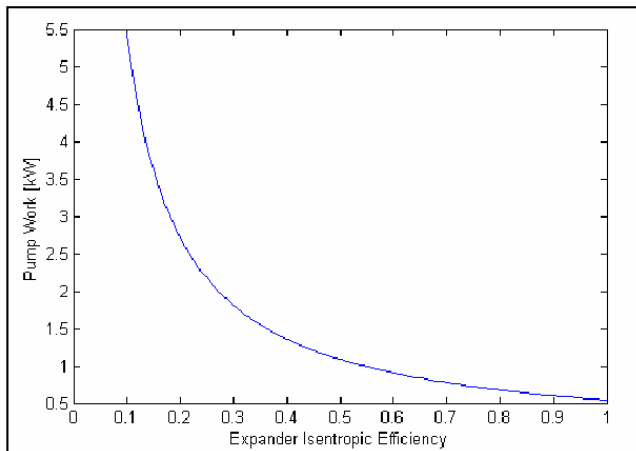


Figure 5.2 Pump work variation with expander efficiency

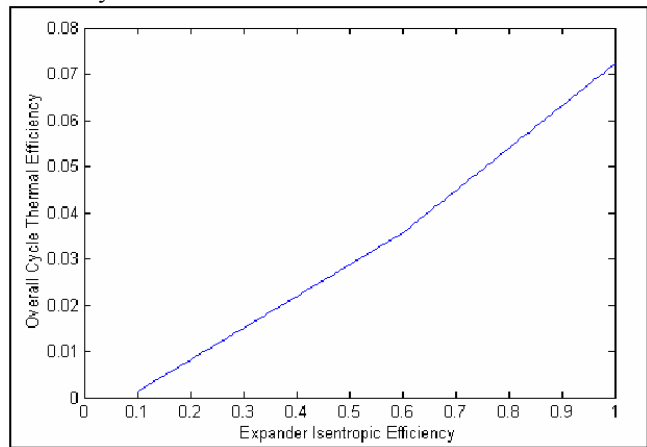


Figure 5.5 Cycle thermal efficiency vs expander efficiency

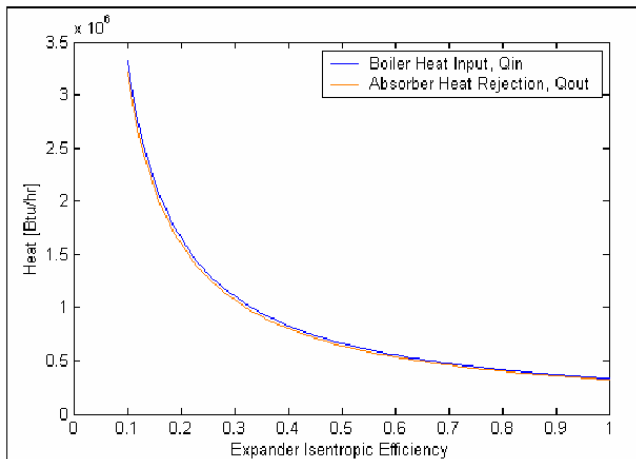


Figure 5.3 Boiler heat input and absorber heat rejection vs. expander efficiency

Thermal efficiency increases linearly with expander efficiency; however, a sudden increase in slope occurs at approximately $\eta_e = 0.6$ at which point the cooling effect begins to enhance the thermal efficiency of the cycle. The highest achievable thermal efficiency for the given operating conditions is 7.22%.

The mass fraction of ammonia entering the expander was analyzed more closely to judge the assumption of pure vapor leaving the rectifier and to determine the impact that trace quantities of water have on the cycle performance. The analysis was carried out for an ideal expander. Figure 5.6 shows the profound negative effect on cooling capacity. The cooling capacity diminishes to zero rapidly as trace amounts of water are introduced into the expander stream up to only 2.5% by mass. Boiler heat input is reduced from 331,566 Btu/hr (97.18 kW) to 320,934 Btu/hr (94.06kW); however, thermal efficiency is reduced 9.26% from 7.22% to 6.55% because of the lost cooling benefit. Another concern is that the expander exhaust temperature drops below the mixture dew point as shown in Figure 5.7. At a 2.5% water vapor concentration by mass, the mixture quality is 0.967. This most likely is not an issue

for compliant devices such as scrolls in which a small quantity of liquid can be tolerated, or with high-speed devices such as turbines, in which the residence time of the fluid is shorter than the time required for condensation to occur (metastable condition).

These results show that rectifier design is a crucial element for the success of a small scale combined cycle in the hydrogen production field in which high efficiency translates into greater liquid yield per unit energy input.

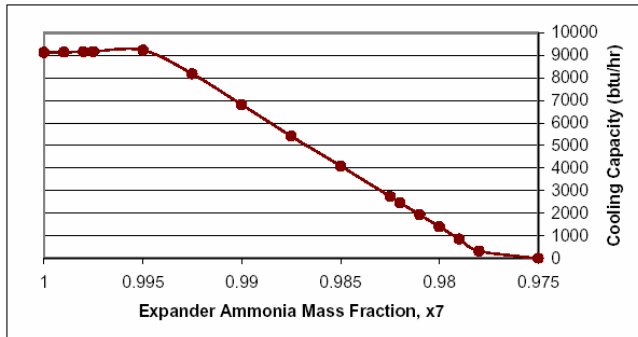


Figure 5.6 Effect of trace amounts of water within in the expander inlet stream cycle cooling capacity

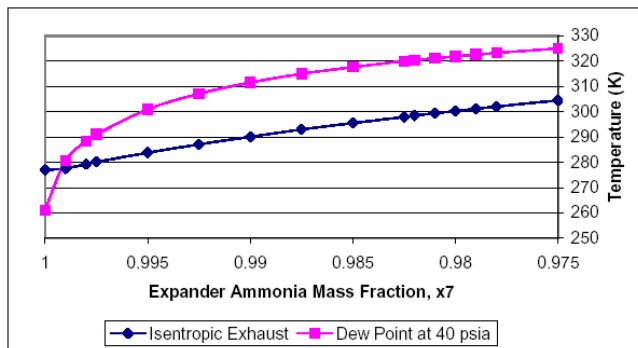


Figure 5.7 Expander exhaust and dew point temperature at several water concentrations

Scroll Expander Performance Study

Scroll expander performance was measured for inlet pressures of 60, 70, and 80 psig; a range suitable for the 5kW combined cycle. Two tests were performed at each pressure to verify repeatability of the results. Tests at pressures over 80 psig were not feasible due to the relatively small tank and the inability of the compressor to supply compressed air at high flow rates (> 60 scfm).

Figure 5.8 shows the results of the repeatability analysis applied to shaft power measurements at 65 psig. The second set of data indicated by the square points agrees well with the trend line of the initial data. beginning at a maximum value and decreasing monotonically with RPM as expected, the power output reaches a maximum at

approximately 1500 RPM before decreasing toward zero in all three cases. This is thought to occur due to choked conditions at the expander exit. Flow becomes choked when the port to fitting area ratio is smaller than the critical area ratio given by the temperature and pressure of the exiting air. The area of the expander exit port and fitting is 0.375” and 0.25”, respectively. Further evidence of choked flow is given by the fact that the maximum attainable rotational speed is only 3000 RPM at source pressures up to 110 psig, whereas the TRS-90 scroll compressor can normally achieve speeds of up to 9000 RPM (Sanden engineer, personal conversation).

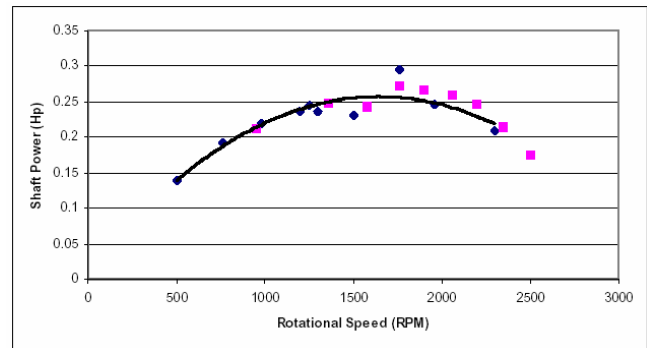


Figure 5.8 Repeatability analysis applied to shaft power output at 65 psig

A similar trend is witnessed with isentropic efficiency, η_e (Figure 5.9). Low values of η_e are attributed to the poor volumetric efficiency, η_v , of the expander at low RPM and relatively high torsional load. Increased torsional resistance raises the pressure within each pocket of the scroll, enhancing tip leakage and reducing volumetric efficiency. Figure 5.10 illustrates the relationship between volumetric efficiency and rotational speed. At each pressure, η_v increases asymptotically toward a final value between 0.8 and 0.9.

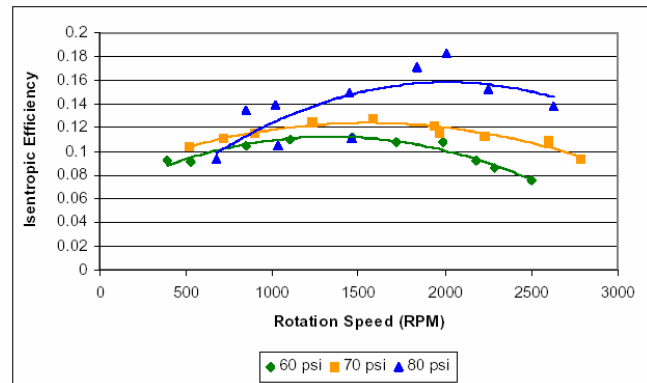


Figure 5.9 Scroll expander isentropic efficiency

The volumetric efficiency indicates the percentage of air that passes through without doing any useful work. This process can be modeled as isenthalpic, with the

approximation of constant temperature (ideal gas). The warmer air mixes with the cold air, from which work was extracted, within the scroll housing effectively raising its temperature prior to the measurement location. Furthermore, heat is exchanged from the surroundings to the fluid through the exit port fittings. This temperature rise causes an erroneous calculation of the exit enthalpy and thus the isentropic efficiency. However, trends may still be observed to determine where the point of maximum efficiency occurs. The exit temperature variation with rotational speed is shown in Figure 5.11. The points of minimum exit temperature coincide with those of maximum power output as expected from the First Law of Thermodynamics.

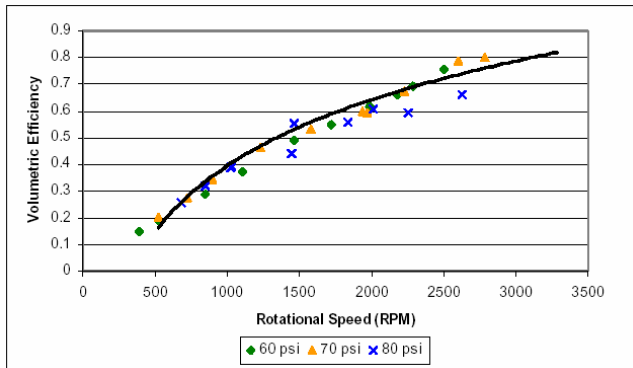


Figure 5.10 Volumetric efficiency variation with expander rotational speed

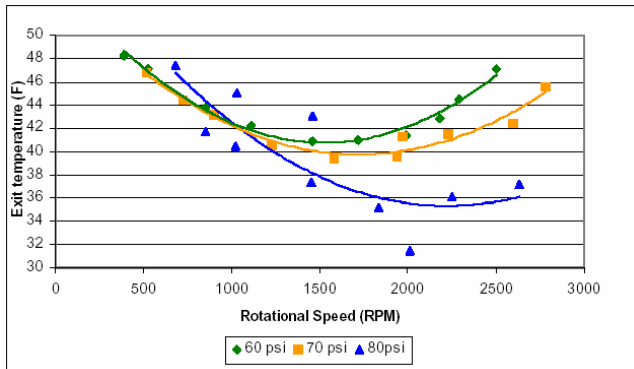


Figure 5.11 Expander exit temperature and rotational speed relationship

The maximum power output of 0.368 Hp (0.274 kW) occurred at 1460 RPM for the 80-psig inlet pressure case. The most efficient operating point is 18.2%. Rotational speed, inlet pressure, and power output at this point is 2000, 80 psig, and 0.282 Hp. The temperature of the working fluid (excluding leakage) is found at any point using the volumetric efficiency and flow rate. Therefore, with a volumetric efficiency of 0.6092 and temperatures of 71.6 °F and 31.5 °F at the inlet and exit at this point, the temperature of the working fluid is 4.77 °F.

The low value of isentropic efficiency is due primarily to leakage caused by the density mismatch. The TRS-90 is designed for R-134A with a density of 0.262

lbm/ft³ at STP whereas the density of air at STP is .07298 lbm/ft³; nearly 3.6 times lower than R-134A, and the density of ammonia is 0.04333 lbm/ft³; 1.6 times lower than air. The performance of the expander with ammonia is expected to be worse than with air because higher pressures are required for a unit volume of ammonia to store an equal amount of energy as a unit volume of air at a given temperature. This relationship is arrived at by considering the ideal gas law as a first approximation.

Higher pressures lead to increased leakage within the scroll and a loss of performance. Additionally, ammonia is a smaller molecule than air and much smaller than R-134A, further facilitating tip leakage and reducing efficiency. Fundamental design changes are required for the scroll concept to be utilized as an expander. The geometry of each scroll element should be altered such that the total number of chambers is increased as shown in Figure 5.12. This design reduces pressure differences between chambers and hence leakage (Hans-Joachim and Radermacher, 2003).

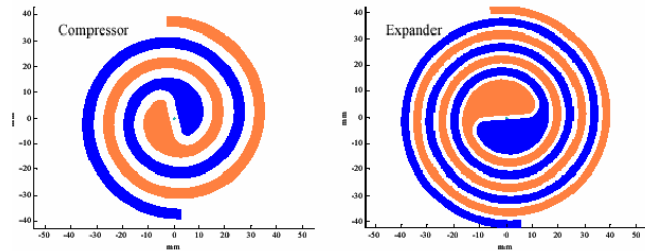


Figure 5.12 Comparison of optimum geometries of a scroll compressor (left) and expander (right) (Adapted from Hans-Joachim and Radermacher, 2003)

6. CONCLUSIONS

Global energy consumption is projected to increase 54% over the next 25 years. With proven oil reserves being called into question beyond 2030 it is important to develop renewable technologies to sustain the future global energy demand. By introducing an alternative fuel for transportation only, oil consumption can be reduced by as much as 20%.

Hydrogen has many characteristics that make it a desirable fuel. It has the highest energy content per unit mass of any known fuel – nearly 3 times higher than gasoline, it burns cleanly and efficiently, and it can be produced from water via electrolysis powered by renewable energy. Two major obstacles to the emergence of a hydrogen economy are the limited means available to efficiently produce mass quantities of hydrogen from renewable energy sources and the storage issues related to the low energy density of hydrogen. Liquefying hydrogen provides a solution to its low density; however, the process requires additional energy.

This work explored the possibility of using an ammonia-based combined power/cooling cycle to produce hydrogen from renewable resources and pre-cool it prior to liquefaction in an effort to reduce the overall energy consumption. The advantage of this cycle is its ability to utilize low temperature heat sources available from solar and geothermal resources.

Simulations of the Claude liquefaction process and the 5-kW ammonia-based combined power/cooling cycle were developed to model the effects of component efficiencies and operating parameters on the maximum hydrogen production rate and system energy requirement. Additionally, a performance test of a scroll compressor was performed to gauge its effectiveness as an expander for the combined cycle.

Conclusions resulting from tests and analyses are summarized below:

1. Pre-cooling hydrogen has little effect on the specific liquefaction energy and is detrimental to the liquefier efficiency.
2. Pressurized electrolysis is the most effective method of reducing the energy consumed in liquefaction.
3. The total energy required to produce and liquefy hydrogen is 28.656 kW-h/lbm-H₂ (63.175 kW-h/kg-H₂); 86% of which is consumed during electrolysis. A maximum of 7.21 gallons (27.3 liters) per day of liquid hydrogen can be produced from a 5-kW combined cycle.
4. The mass flows as well as the heat and work interactions of the 5-kW combined cycle scale with inverse of expander efficiency ($1/\eta_e$). Sixty percent expansion efficiency is required to extract cooling from the cycle.
5. Cooling capacity of the cycle is extremely sensitive to the vapor mass fraction of the expander inlet stream. At 2.5% water by mass and for perfect expansion, the cooling capacity completely diminishes.
6. Results of the performance test indicate that scroll compressors operate poorly as expanders. Low isentropic efficiencies result from leakage around the scroll tips. Improvements in the scroll design such as increasing the wrap of each scroll element and using low-friction material for oil-less operation would make the scroll an efficient expansion device suitable for the combined cycle.

REFERENCES

Clean Energy Research Center, 2003, "Journey to Sustainable Energy: The H₂ Solution," University of South Florida, Tampa, FL. <http://www.cerc.eng.usf.edu>, last accessed: 11/2004.

Copeland Corp., 2001, "Scroll Compressor Technology and Air Conditioning, Heat Pump, and Refrigeration Applications," *Vi Ibero-American Congress of Air Conditioning and Refrigeration*, Available at <http://www.copelandcorp.com/americas/news/news004.htm/scroll-english.pdf>

Energy Information Administration, 2003, "Annual Energy Review 2003," DOE/EIA – 0384(2003), Washington, DC.

<http://www.eia.doe.gov/emeu/aer/contents.html>, last accessed: 11/2004.

Energy Information Administration, 2004, "International Energy Outlook 2004," Washington, DC. Available at <http://www.eia.doe.gov/oiaf/ieo/world.html>, last accessed: 11/2004.

Flynn, T. M., 1997, *Cryogenic Engineering*, Marcel Dekker, New York.

Fuel Cell Store, 2003, "Hydrogen Storage," Boulder, CO. http://www.fuelcellstore.com/information/hydrogen_storage.html, last accessed: 11/2004.

Goswami, D. Y., 1995, "Solar Thermal Power: Status of Technologies and Opportunities for Research," *Heat and Mass Transfer 95, Proceedings of the 2nd ASME-ISHMT Heat and Mass Transfer Conference*, Tata-McGraw Hill Publishers, New Delhi, India, pp. 57 – 60.

Gravesen, J., Henriksen, C., 2001, "The Geometry of the Scroll Compressor," *SIAM Review*, Vol. 43, No. 1, pp. 113-126.

Hans-Joachim, H., Radermacher, R., 2003, *CO2 Compressor-Expander Analysis: Final Report*, Air-Conditioning and Refrigeration Technology Institute, Arlington, VA, ARTI-21CR/611-10060-01.

Hasan, A. A., Goswami, D. Y., 2003, "Exergy Analysis of a Combined Power and Refrigeration Thermodynamic Cycle Driven by a Solar Heat Source," *ASME Journal of Solar Energy Engineering*, Vol. 125, No. 1, pp. 55 – 60.

Mirabal, S. T., 2003, "An Economic Analysis of Hydrogen Production Technologies Using Renewable Energy Resources," Master's thesis, University of Florida.

National Hydrogen Association, 2004, "Hydrogen FAQs," Washington, DC. <http://www.hydrogenus.com/h2-FAQ.asp>, last accessed: 11/2004.

Ramsay, W. C., 2003, *Public-Private Dialogue, International Partnership for a Hydrogen Economy*, International Energy Agency, Paris.

Schein, C., Radermacher, R., 2001, "Scroll Compressor Simulation Model," *ASME Journal of Engineering for Gas Turbines and Power*, Vol. 123, pp. 217 – 225.

Sunattech Inc., 2001, *IEA Agreement on the Production and Utilization of Hydrogen, Task 12: Metal Hydrides and Carbon for Hydrogen Storage, Executive Summary*, edited by Sandrock, U.S. Department of Energy, Washington, DC.

Tamm, G., Goswami, D. Y., Lu, S., Hasan, A., "A Novel Combined Power and Cooling Thermodynamic Cycle for Low Temperature Heat Sources – Part I: Theoretical Investigation," *ASME Journal of Solar Energy Engineering*, Vol. 125, No. 2, np.

Wells, D. N., 2000, "Scroll Expansion Machines for Solar Power and Cooling Systems," *Proceedings of Solar 2000*, American Society of Mechanical Engineers, Madison, WI, np.